Charge-transfer optical absorption in linear magnetic insulators in a strong electric field

S. K. Lyo
Sandia National Laboratories, Albuquerque, New Mexico 87185
(Received 8 July 1985)

The effect of a strong electric field on the charge-transfer optical absorption is studied in linear narrow-band Mott-Hubbard insulators (or semiconductors) such as alkali-TCNQ's (tetracyanoquinodimethanes) and antiferromagnetic Heisenberg chains, using the half-filled-band Hubbard model with strong on-site Coulomb repulsion. It is shown that, for an antiferromagnetic ground state, the main effect of the field is to severely (i.e., nonlinearly with the applied field) squeeze the unperturbed continuum absorption band into a narrower band of unevenly spaced discrete rungs of a Stark ladder. The intensity of the absorption into the Stark-ladder states has exponential tails both above and below the main band, showing a discrete version of the Franz-Keldysh effect. For random and ferromagnetic spin configurations, the absorption profile narrows and the discrete absorption resonances smear into sharp continuum structures.

I. INTRODUCTION

A number of years ago Wannier[1] proposed that electronic states in crystalline solids form Stark ladders in a strong electric field. Since then a large number of authors have studied this subject.[1–4] Theoretical works,[1–4] which include optical-absorption studies,[3] have been limited to non-interacting-electron systems so far. Experimentally, despite the numerous efforts such as optical absorption,[5] as well as other electronic-transport studies[4] in ordinary semiconductors aimed at discovering Stark ladders in the past, there has been no conclusive evidence of their existence. In this paper we propose the possibility of observing Stark ladders and the Franz-Keldysh effect[6] in the charge-transfer optical-absorption spectrum of a new class of systems, namely one-dimensional narrow-band Mott-Hubbard magnetic insulators (or semiconductors). For this purpose we study the optical-absorption line shape, using a half-filled-band Hubbard model[7] with a large on-site Coulomb repulsion. The advantage of these systems over the ordinary semiconductors studied previously experimentally lies in the facts that the transverse degree of freedom of electrons which masks the Stark structures are absent and that the narrow band makes the effect of the field more pronounced. The systems suitable for such studies are, for example, linear charge-transfer organic salts such as alkali-TCNQ's (tetracyanoquinodimethane) (Refs. 8—11) and possibly spin-$\frac{1}{2}$ linear-chain antiferromagnetic Heisenberg systems such as α-CuNSal [α-bis (N-methylsalicylaldiminato)copper(II)] (Ref. 12). From a practical point of view, such studies are expected to give additional information on charge-transfer absorption in organic conductors, which has been an important tool for looking into electronic structures and Coulomb interactions.[8–11] Also, the optical absorption depends sensitively on the spin configuration of the electronic ground-state manifold and is expected to yield valuable information on the spin states of linear antiferromagnetic Heisenberg systems.

II. MODEL

The system is described by the model Hamiltonian[7]

$$H = H_0 + V \,, \tag{1a}$$

with

$$H_0 = U\sum_m n_{m,\uparrow} n_{m,\downarrow} + \epsilon \sum_\sigma m n_{m,\sigma} \tag{1b}$$

and

$$V = -t\sum_{m,\sigma} (a^\dagger_{m+1,\sigma} a_{m,\sigma} + a^\dagger_{m,\sigma} a_{m+1,\sigma}) \,. \tag{1c}$$

Here, $a^\dagger_{m,\sigma}$ ($a_{m,\sigma}$) creates (destroys) a state of spin σ at site m, $n_{m,\sigma}$ ($= a^\dagger_{m,\sigma} a_{m,\sigma}$) is the number operator, and $n_m = n_{m,\uparrow} + n_{m,\downarrow}$. The quantities t and ϵ (>0) denote the transfer integral and the rise of the electronic potential energy over a unit lattice constant "a" due to a uniform electric field along the chain direction, respectively.

In the limit $t/U \ll 1$ and at low temperatures $T \ll U/k_B$ (k_B is Boltzmann's constant), the absorption arises from exciting an electron from the lower Hubbard band[7] with one electron per site into the upper band, generated by moving a hole and an adjacent doubly occupied site (to be referred to as a particle) by applying V successively without recombination. Such an approximation is relevant, for example, to K-TCNQ, where $U \times 1.4$ eV $\gg 4t \times 0.3$ eV.[11] The absorption spectrum is given by the real part of the conductivity $\sigma_R(\omega)$, which is evaluated by Kubo's formula.

In previous papers[13,14] we have studied optical absorption for the Hamiltonian in (1) in the absence of an external field (i.e., $\epsilon = 0$). In an external field corresponding to ϵ, the hole and particle have effective interaction $\pm m\epsilon$ at a separation of ma depending on whether the particle is on the right side ($+$) or on the left side ($-$) of the hole. The absorption is found in this case by extending the method of Ref. 14 in a straightforward way, yielding

$$\sigma_R(\omega)=\tfrac{1}{2}p\sigma_0\int_0^1 Q(x,p)[\rho_+(\omega,x)+\rho_-(\omega,x)]dx\ , \tag{2a}$$

where

$$\sigma_0=\frac{2pq^2N\pi}{\Omega\omega}\left[\frac{ta}{\hbar}\right]^2 . \tag{2b}$$

In (2), $Q(x,p)$ is a normalized distribution function

$$Q(x,p)=\frac{2(1-p^2)}{\pi(1-x^2)^{1/2}[(1+p)^2-4px^2]}\ , \tag{3}$$

and $\rho_\pm(\omega,x)$ is the normalized particle-hole density of states

$$\rho_\pm(\omega,x)=\frac{1}{\pi}\mathrm{Im}\left\langle 0,\pm1\left|\frac{1}{\hbar\omega-H_0-H'}\right|0,\pm1\right\rangle . \tag{4}$$

Here, ω contains an infinitesimally small negative imaginary part and Im means the imaginary part. The quantities q, N, and Ω in (2) represent the electronic charge, the total number of lattice sites, and the sample volume, respectively. The intensity satisfies a sum rule $\int\sigma_R(\omega)d\omega=\sigma_0$. In (4), $|0,\pm1\rangle$ designates an antiferromagnetic state vector with a hole at $m=0$ and a particle at $m=\pm1$.[13] Only these state vectors have nonvanishing transition dipole matrix elements. The operator H' is of the same form as V, except that it transfers only the particle between adjacent sites with a matrix element $t'=2tx$, while the particle and the hole are forbidden to occupy a same site. The factor 2 in the expression of the effective transfer integral t' amounts to doubling of the absorption bandwidth due to the additional hole degree of freedom. This is analogous to the fact that in an ordinary semiconductor the optical bandwidth equals the sum of the valence- and conduction-band widths. The factor x in the expression of t' indicates that the effective transfer integral t' has a distribution between zero and $2t$ according to the function $Q(x,p)$. This function is determined by the spin-configuration factor p.[13,14] The latter is defined in such a way that the probability of having k consecutive spins to the right (or left) of the hole in an antiferromagnetic arrangement equals p^k. We have $p=1$, $\frac{1}{2}$, and 0 for antiferromagnetic, random, and ferromagnetic spin configurations, respectively.

For an antiferromagnetic ground state we have $Q(x,p)=\delta(x-1+0)$ (0 is a positive infinitesimal) and the the variable x is replaced by unity in (2a). The role of $Q(x,p)$ is then to transform the absorption of a system with an arbitrary spin configuration p into a sum of contributions from an infinite number of antiferromagnetic spin states with a continuous distribution of effective transfer integrals; while the wave functions for the excited upper Hubbard-band manifold depend on the spin configuration in a complicated way, a simple coherent single-particle picture is available for the antiferromagnetic configuration for this many-body problem.[13,14] We discuss this simple and important situation first in the following, postponing the more complex cases of random and ferromagnetic spin configurations until Sec. V.

III. ANTIFERROMAGNETIC GROUND STATE

The quantity $\rho_\pm$ in (4) is the particle-hole local density of states at a separation of a unit lattice constant: Namely it is the probability that the particle and the hole are at a distance a averaged over all particle-hole eigenstates. The problem is then equivalent to that of a semi-infinite tight-binding chain extending from $m=1$ to $m=\infty$:

$$uc_m=-2t(c_{m-1}+c_{m+1})\pm m\epsilon c_m\quad(m>0)\ , \tag{5}$$

with $u=\hbar\omega-U$ and with a vanishing amplitude at $m=0$ (i.e., $c_0=0$). The subscript m denotes the separation between the particle and the hole. The upper (lower) sign in (5) corresponds to ρ_+ (ρ_-) and to the situation where the particle is created at the high- (low-) energy side of the hole. It is sufficient to consider only the upper sign, because there is a simple relationship between ρ_+ and ρ_-, as will be shown later. The solution of (5) that converges for large m is $c_m\sim J_{m-u/\epsilon}(4t/\epsilon)$, where $J_\nu(z)$ is the Bessel function of order ν. The eigenvalues are determined by the condition $c_0=0$ (Ref. 2):

$$J_{-u/\epsilon}(4t/\epsilon)=0\ . \tag{6}$$

An alternative approach is to express $\rho_\pm$ in (4) in continued fractions. This is achieved by rewriting the Green's function in (4) in terms of forward-going self-energies:[15]

$$\rho(u,\pm\epsilon)\equiv\rho_\pm(\omega,1)=\frac{1}{\pi}\mathrm{Im}\left[\frac{1}{u-(\pm\epsilon)-\Sigma_1}\right]\ , \tag{7a}$$

with

$$\Sigma_m=\frac{(2t)^2}{u-(\pm)(m+1)\epsilon-\Sigma_{m+1}}\ . \tag{7b}$$

The continued fraction in (7) is rewritten as[16]

$$\rho(u,\epsilon)=-\frac{1}{2\pi t}\mathrm{Im}\left[\frac{J_{1-u/\epsilon}(4t/\epsilon)}{J_{-u/\epsilon}(4t/\epsilon)}\right] . \tag{8}$$

The poles of the expression in (8) are then determined by (6). The properties of ρ_- are related to those of ρ_+ by

$$\rho(u,-\epsilon)=\rho(-u,\epsilon)\ . \tag{9}$$

Namely, the eigenvalues of ρ_- have opposite signs of those of ρ_+. In the following we discuss only ρ_+ for convenience and measure the energy in units of the bandwidth (i.e., $4t=1$).

In the absence of the field, the self-energy Σ_m in (7) does not depend on the site index m, yielding[13]

$$\rho(u,0)=\begin{cases}(2/\pi)(1-u^2)^{1/2} & \text{for } -1\leqq u\leqq 1\ ,\\ 0 & \text{otherwise}\ .\end{cases} \tag{10}$$

The absorption width equals twice the bandwidth and the intensity is maximum at the center.

Practically, the energy ϵ is much smaller than the bandwidth (i.e., $\epsilon\ll1$), even for a strong field. For a field of 100 kV/cm and $a=4$ Å, for example, we have $\epsilon=0.02$ for a bandwidth 0.2 eV. One might expect a small linear positive (negative) shift $\sim\epsilon$ ($-\epsilon$) for ρ_+ (ρ_-) for the exci-

tation threshold from the unperturbed position $u=-1$ $(+1)$ in (10). Interestingly, we find a nonlinearly large shift $\sim\epsilon^{2/3}$. For example, for a field corresponding to $\epsilon=0.05$, we find a shift as large as 0.25. This shift is clearly seen in the position (at -0.75) of the first spike (corresponding to the first rung of the Stark ladder) in Fig. 1, where a histogram representation of $\rho(u,\epsilon=0.05)$ is displayed as a function of u. The absorption is obtained numerically by iteration from the continued-fraction representation in (7). A more detailed description of the numerical method will be given later. The spikes correspond to a series of delta functions spread out over an energy-bin width $\Delta u=0.01$: The total area (i.e., intensity) of the spikes equals unity.

In a strong field, an electron (i.e., the particle) as well as a hole with a maximum kinetic energy ~ 1 is expected to be localized within a range $\sim a/\epsilon$. The eigenvalues for $\rho(u,\epsilon)$ become discrete, forming a Stark ladder: The spacing between rungs become gradually narrow, reaching an asymptotic value ϵ approximately for $u-1>\epsilon^{2/3}$. For the eigenvalues corresponding to these evenly spaced rungs (Fig. 1), the eigenfunctions are localized far away from the chain end. Only those eigenfunctions with energies in the unperturbed absorption band $-1<u<1$ have significant amplitudes at $m=1$ and transition dipole matrix elements. Nevertheless, Stark states immediately outside this band have small but non-negligible amplitudes giving rise to visible absorption tails. In Fig. 2 we display the total absorption

$$\sigma_R(u)/\sigma_0=\tfrac{1}{2}[\rho(u,\epsilon)+\rho(-u,\epsilon)]$$

as a function of u for $\epsilon=0.05$ and compare it with the absorption in the absence of the field (solid curve) given by (10). It is seen that the effect of the field is to squeeze the unperturbed continuum absorption band into a narrower band of discrete excitations with exponentially decaying

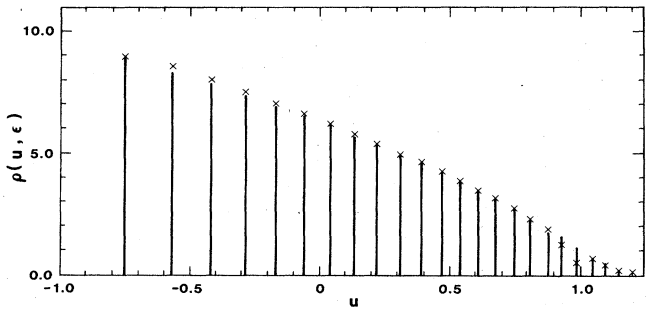

FIG. 1. Histogram representation of the normalized optical density $\rho(u,\epsilon)$ [defined in (7a)] for a potential-energy rise over a unit lattice constant $\epsilon=0.05$ and for an antiferromagnetic spin configuration as a function of the excitation energy $u=\hbar\omega-U$. The bandwidth $(4t)$ is defined as unity. The width of the bins (spikes) equals 0.01. The crosses represent analytical results [Eqs. (11)–(13)] for the excitation energies and the intensities spread over the same bin size for comparison with the histogram.

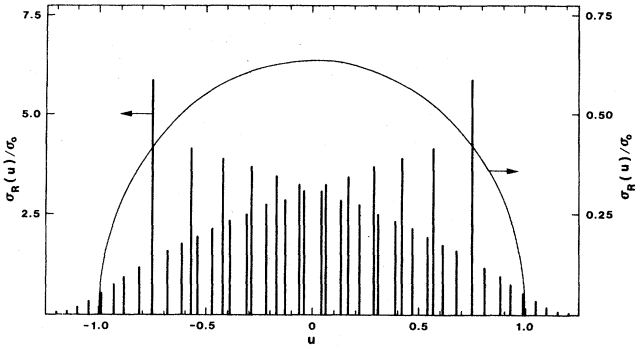

FIG. 2. Histogram representation (left scale) of the normalized total absorption $\sigma_R(u)/\sigma_0=[\rho(u,\epsilon)+\rho(-u,\epsilon)]/2$. The quantity $\rho(u,\epsilon)$ is given by the histogram in Fig. 1. The solid curve indicates the unperturbed absorption in the absence of an external dc field.

discrete absorption tails both above and below the unperturbed band (i.e., $|u|>1$).

In the following we evaluate analytically the excitation energies and the normalized optical density $\rho(u,\epsilon)$ in the asymptotic limit $\nu=|u|/\epsilon\to\infty$, using asymptotic forms of $J_\nu(\alpha\nu)$ and

$$J_{-\nu}(\alpha\nu)=J_\nu(\alpha\nu)\cos(\pi\nu)-Y_\nu(\alpha\nu)\sin(\pi\nu)\ ,$$

where $\alpha=|u|^{-1}$. In the region $u\ll-\epsilon$, the zeros of (6) are given by

$$(1-u^2)^{1/2}+u\cos^{-1}(-u)=\pi\epsilon(m+\tfrac{3}{4})\ , \tag{11a}$$

where m is any integer in the range $0\leqq m\leqq 1/\pi\epsilon-\frac{3}{4}$. For $\epsilon=0.05$, for example, the allowed quantum numbers are $m=0,1,\ldots,5$. Equation (11a) is solved approximately, yielding[2]

$$u_m=-1+\left[\frac{3\pi\epsilon}{2\sqrt{2}}\right]^{2/3}(m+\tfrac{3}{4})^{2/3}\ . \tag{11b}$$

These solutions are very accurate when the second term on the right-hand side of (11b) is small. The latter equals $(9\pi\epsilon/8\sqrt{2})^{2/3}$ for $m=0$. This quantity is the field-induced shift of the excitation threshold for ρ_+ discussed earlier. The absorption intensity is obtained from (8) and is approximately equal, in the region $2\epsilon\ll-u(1-u^2)$ (i.e., away from $u=0$ and -1), to

$$\rho(u,\epsilon)=\frac{2\epsilon(1-u^2)^{1/2}}{\cos^{-1}(-u)}\delta(u-u_m)\ . \tag{11c}$$

The six excitation energies $(m=0,1,\ldots,5)$ determined from (11a) for $\epsilon=0.05$ are marked as crosses in Fig. 1 in the negative-energy $(u<0)$ region. The heights indicate the strengths of the delta functions of (11c) spread out to the same width $\Delta u=0.01$ for comparison with the numerical histogram. The approximate expression in (11b) gives a similar result. The agreement is excellent.

In the region $\epsilon\ll u<1$, the roots of (6) are determined by

$$u_m+\frac{1}{\pi}[(1-u^2)^{1/2}-u_m\cos^{-1}u_m]=\epsilon(m-\tfrac{1}{4}) , \quad (12a)$$

where m are integers in the range $1/\pi\epsilon+\frac{1}{4}\leqq m \leqq 1/\epsilon+\frac{1}{4}$. For $\epsilon=0.05$, the allowed quantum numbers are $m=7,8,\ldots,20$. In the neighborhood of $u_m\sim 1$, the second term on the left-hand side of (12a) is small and the eigenvalues $u_m\approx\epsilon(m-\frac{1}{4})\approx\epsilon m$ begin to form a Stark ladder. The absorption intensity is approximately given, in the region $2\epsilon\ll u(1-u^2)$ (i.e., away from $u=0$ and 1), by

$$\rho(u,\epsilon)=\frac{2\epsilon(1-u^2)^{1/2}}{\pi-\cos^{-1}u}\delta(u-u_m) . \quad (12b)$$

The 14 excitation energies ($m=7,8,\ldots,20$) and intensities for $\epsilon=0.05$ determined from (12) are marked as crosses in the region $0<u<1$. The agreement with the histogram is very good, except very near $u=1$.

In the region $u=1+u'$ with $u'\gg\epsilon^{2/3}$, the excitation energies form a Stark ladder:

$$u_m=m\epsilon , \quad (13a)$$

where m is an integer. The absorption has an exponential tail:

$$\rho(u,\epsilon)=\frac{\epsilon}{\pi}\left[\frac{1}{u-1}+\frac{5}{3}\right][2(u-1)]^{3/2} \times\exp\left[-\frac{2u}{3\epsilon}[2(u-1)]^{3/2}\right]\delta(u-m\epsilon) . \quad (13b)$$

This result corresponds to the Franz-Keldysh effect.[6] However, in contrast to a wide-band semiconductor, where the relevant continuum tail is inside the band gap, we expect that discrete tails should be observed both above (ρ_+) and below (ρ_-) the absorption band in the present one-dimensional narrow-band systems. The predictions of (13) are marked as crosses in Fig. 1 for $\epsilon=0.05$ and for $u>1$, again yielding excellent agreement with the numerical results.

For eigenfunctions with $u\gg 1$ the particle and hole are very much separated and the absorption is negligibly small:

$$\rho(u,\epsilon)=\frac{\epsilon}{\pi}\left[\frac{e}{2u}\right]^{2u/\epsilon}\delta(u-m\epsilon) . \quad (14)$$

In (14), e is the natural number.

IV. NUMERICAL ANALYSIS

The optical density $\rho(u,\epsilon)$ in (7a) can be easily evaluated numerically by iteration as was mentioned earlier: For large m we approximate $\Sigma_m=\Sigma_{m+1}$ in (7a), obtaining

$$\Sigma_m=\tfrac{1}{2}[z-\mathrm{sgn}(z)(z^2-1)^{1/2}] , \quad (15)$$

with $z=u+(m+1)\epsilon$. Starting from a large number $m=M$ for the self-energy in (15), we apply (7b) repeatedly to find Σ_0, which is related to ρ by $\rho(u,\epsilon)=\Sigma_0/4\pi$. For an actual numerical evaluation we use $M=200$ and assign a small negative imaginary part $\delta=5\times10^{-4}$ to u. We evaluate $\rho(u,\epsilon)$ at energy intervals of $\Delta u=10^{-4}$ and sum the intensity in bins of size 10^{-2} (Fig. 1). The total intensity in each spike is obtained by multiplying its height by the bin size 10^{-2}. The same result is obtained if we double M and reduce δ and Δu by half, indicating that the numerical error is small. Furthermore, the total calculated intensity is unity, as required by the sum rule, indicating that every excitation is accounted for in the numerical analysis.

A more efficient method of obtaining $\rho(u,\epsilon)$ is to evaluate the poles and residues of the expression in (8) by using a library routine. This method leads to the same result as that displayed in Fig. 1.

V. RANDOM AND FERROMAGNETIC SPIN CONFIGURATIONS

The spin state of the lower Hubbard band (with one electron per site) has a random spin configuration at high temperatures and a ferromagnetic spin arrangement in a high magnetic field. The spin state can readily be controlled because the exchange energy $\sim t^2/U$ is small. The optical absorption for these spin configurations is obtained from (2) and (7)—(9) by replacing t in (8) by xt and integrating over x between 0 and 1 with the weighting function $Q(x,p)$. As a result, the effective absorption width becomes narrower for smaller p. The discrete absorption energies smear into sharp continuum peaks. Also, the intensity σ_0 decreases linearly with p. This effect is clearly seen in Figs. 3 and 4, where the normalized absorption σ_R/σ_0 (solid curves) is plotted as a function of u for the lower half of the absorption band (i.e., $u<0$) for random spin configuration ($p=\frac{1}{2}$) and the ferromagnetic

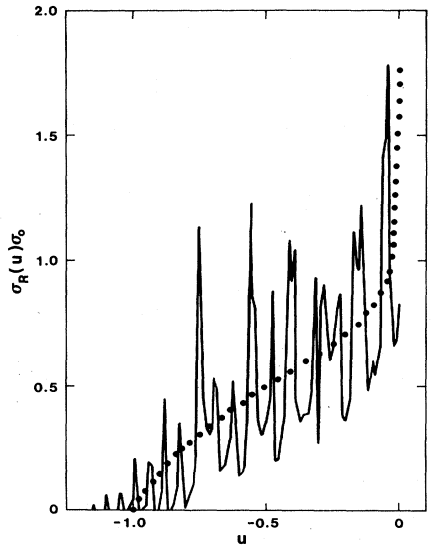

FIG. 3. Lower half ($u<0$) of the normalized absorption intensity $\sigma_R(u)/\sigma_0$ [defined in Eq. (2)] for a potential-energy rise over a unit lattice constant $\epsilon=0.05$ and for a random spin configuration as a function of the excitation energy $u=\hbar\omega-U$ in units of the bandwidth ($4t$). The dotted curve indicates the absorption in the absence of an external field.

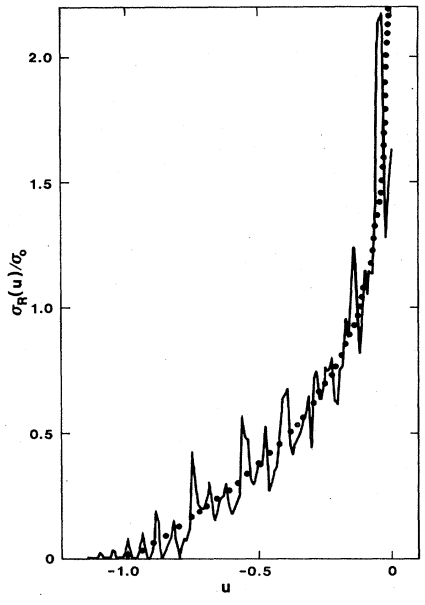

FIG. 4. Lower half ($u<0$) of the normalized absorption intensity $\sigma_R(u)/\sigma_0$ [defined in Eq. (2)] for a potential-energy rise over a unit lattice constant $\epsilon=0.05$ and for a ferromagnetic spin configuration as a function of the excitation energy $u=\hbar\omega-U$ in units of the bandwidth ($4t$). The dotted curve indicates the absorption in the absence of an external field.

configuration ($p=0$), respectively. Also, absorptions in the absence of an external field are displayed by dotted curves for comparison. The upper half of the band not shown is the mirror image of the lower half with respect to $u=0$ [i.e., $\sigma_R(-u)=\sigma_R(u)$]. The results (solid curves) in Figs. 3 and 4 are obtained numerically by evaluating the poles and residues of the expression in (8) through a library subroutine. The accuracy of the results was checked by ensuring that the sum rule is satisfied.

VI. CONCLUSIONS

We have examined the charge-transfer optical absorption in a strongly correlated half-filled Hubbard band[7] in a strong electric field. For an antiferromagnetic ground state the unperturbed (i.e., field-free) continuum absorption band narrows into a band of intense sharp discrete absorption resonances in a strong field. Franz-Keldysh—type[6] discrete tail absorption into Stark-ladder states is obtained both above and below the unperturbed band. For random and ferromagnetic spin configurations the absorption intensity diminishes. The line shape narrows and the discrete absorption resonances smear into sharp continuum structures. The result is applicable to charge-transfer organic conductors such as alkali-TCNQ's with a Mott-Hubbard insulating ground state[8–11] and possibly to spin-$\frac{1}{2}$ linear antiferromagnetic Heisenberg chain systems such as α-CuNSal.[12]

In this paper long-range Coulomb interaction is ignored. As a result, the absorption line shape is symmetric. Inferring from a previous result of the author,[14] even a weak long-range Coulomb interaction is expected to deform the absorption profile significantly by transferring the intensity from the high-energy region to the low-energy region and to new exciton absorptions in the gap.

ACKNOWLEDGMENTS

The author thanks Dr. D. E. Amos for his kind and indispensable help with the mathematical and numerical aspects of this work. This work was supported by the U.S. Department of Energy under Contract No. DE-AC04-76DP00789.

[1]G. H. Wannier, *Elements of Solid State Theory* (Cambridge University Press, Cambridge, 1960), p. 193; M. Saitoh, J. Phys. C **6**, 3255 (1973); S. Nagai and J. Kondo, J. Phys. Soc. Jpn. **49**, 1255 (1980).

[2]H. Fukuyama, R. A. Bari, and H. Fogedby, Phys. Rev. B **8**, 5579 (1973).

[3]A. Rauh and G. H. Wannier, Solid State Commun. **15**, 1239 (1974); J. Callaway, Phys. Rev. **130**, 549 (1963); **134**, A998 (1964).

[4]A. M. Berezhkovskii and A. A. Ovchinnikov, Phys. Status Solidi (B) **117**, 289 (1983), and references therein.

[5]R. W. Koss and L. M. Lambert, Phys. Rev. B **5**, 1479 (1972).

[6]W. Franz, Z. Naturforsch. **13a**, 484 (1958); L. V. Keldysh, Zh. Eksp. Teor. Fiz. **34**, 1138 (1958) [Sov. Phys.—JETP **7**, 788 (1958)].

[7]J. Hubbard, Proc. R. Soc. London, Ser. A **276**, 238 (1963); **281**, 401 (1965).

[8]S. K. Khanna, A. A. Bright, A. F. Garito, and A. J. Heeger, Phys. Rev. B **10**, 2139 (1974).

[9]J. B. Torrance, B. A. Scott, and F. B. Kaufman, Solid State Commun. **17**, 1369 (1975).

[10]D. B. Tanner, C. S. Jacobsen, A. A. Bright, and A. J. Heeger, Phys. Rev. B **16**, 3283 (1977).

[11]K. Yakushi, T. Kusaka, and H. Kuroda, Chem. Phys. Lett. **68**, 139 (1979).

[12]L. J. Azevedo, A. Narath, P. M. Richards, and Z. G. Soos, Phys. Rev. B **21**, 2871 (1980), and references therein.

[13]S. K. Lyo and J. P. Gallinar, J. Phys. C **10**, 1693 (1977).

[14]S. K. Lyo, Phys. Rev. B **18**, 1854 (1978).

[15]W. F. Brinkman and T. M. Rice, Phys. Rev. B **2**, 1324 (1970).

[16]*Handbook of Mathematical Functions*, edited by M. Abramowitz and I. A. Stegun (Dover, New York, 1972), p. 363.